Three-point susceptibilities $\chi_n(k;t)$ and $\chi_n^s(k;t)$: Mode-coupling approximation

Grzegorz Szamel and Elijah Flenner

Department of Chemistry, Colorado State University, Fort Collins, Colorado 80523, USA

Recently, it was argued that a three-point susceptibility equal to the density derivative of the intermediate scattering function, $\chi_n(k;t)=dF(k;t)/dn$, enters into an expression for the divergent part of an integrated four-point dynamic density correlation function of a colloidal suspension [Berthier *et al.*, J. Chem. Phys. **126**, 184503 (2007)]. We show that, within the mode-coupling theory, the equation of motion for $\chi_n(k;t)$ is essentially identical as the equation of motion for the $\mathbf{q}\rightarrow 0$ limit of the three-point susceptibility $\chi_{\mathbf{q}}(\mathbf{k};t)$ introduced by Biroli *et al.* [Phys. Rev. Lett. **97**, 195701 (2006)]. We present a numerical solution of the equation of motion for $\chi_n(k;t)$. We also derive and numerically solve an equation of motion for the density derivative of the self-intermediate scattering function, $\chi_n^s(k;t)=dF^s(k;t)/dn$. We contrast the wave vector dependence of $\chi_n(k;t)$ and $\chi_n^s(k;t)$.

I. INTRODUCTION

While it has been generally accepted for quite some time that upon approaching the glass transition the liquid's dynamics become increasingly heterogeneous [1], theoretical descriptions of various four-point correlation functions which quantify dynamic heterogeneity have been scarce [2,3]. It has been only in the last few years that a number of different theoretical approaches to this problem appeared [4–10]. According to one of these approaches [8,9], the divergent part of a four-point dynamic density correlation function, integrated over the whole space, can be expressed in terms of so-called three-point susceptibilities. These susceptibilities are defined as the derivatives of the usual two-point correlation function, i.e., the intermediate scattering function, with respect to the densities of the conserved quantities. In the case of a colloidal system there is only one conserved quantity, the number of particles, and thus there is only one susceptibility, the density derivative of the intermediate scattering function.

The first goal of this note is to derive the equation of motion for this susceptibility within the mode-coupling approximation [11–13] and to present numerical solutions of this equation. Not surprisingly, the equation of motion for the density derivative of the intermediate scattering function is essentially identical to that for the long-wave vector limit of the three-point susceptibility introduced by Biroli *et al.* [6]. The latter susceptibility was defined as the derivative of the intermediate scattering function with respect to an external, inhomogeneous potential.

It should be noted that while most theoretical approaches consider the full (i.e., *collective*) four-point dynamic density correlation function, in computer simulations usually the self-part of this function is monitored [14]. For this reason, while discussing the wave vector dependence of dynamic heterogeneities, Berthier *et al.* used a three-point susceptibility equal to the density derivative of the self-intermediate scattering function (see Ref. [9], Sec. II C). Parenthetically, in this way they introduced a somewhat *ad hoc* extension of their theoretical approach. The approach of Berthier *et al.*, at least as presented in Refs. [8,9], is only applicable to the full four-point function.

The second goal of this note is to derive and numerically solve the equation of motion for the density derivative of the self-intermediate scattering function within the mode-coupling approximation, and to contrast the time and wave vector dependence of the density derivatives of the collective and self-intermediate scattering functions. In Ref. [9] the density derivative of the self-intermediate scattering function was calculated by solving the mode-coupling equation of motion for this function at different densities and then performing a numerical differentiation. Numerical solution of the equation of motion for the density derivative of the self-intermediate scattering function allows us to investigate the wave vector at which, according to Berthier *et al.* [8,9], the dynamics of a glassy colloidal suspension is maximally heterogeneous.

II. EQUATIONS OF MOTION FOR $\chi_n(k;t)$ AND $\chi_n^s(k;t)$

We consider the simplest possible model of a colloidal suspension: a system of interacting Brownian particles. Our first object of interest is a three-point susceptibility $\chi_n(k;t)$ which is defined as the density derivative of the intermediate scattering function,

$$\chi_n(k;t) = \frac{dF(k;t)}{dn}. \tag{1}$$

Here $F(k;t)$ denotes the intermediate scattering function,

$$F(k;t) = \frac{1}{N}\langle n(\mathbf{k};t)n(-\mathbf{k})\rangle, \tag{2}$$

where N is the number of particles, $n(\mathbf{k};t)$ is the Fourier transform of the microscopic density at time t, and $n(\mathbf{k})$ $\equiv n(\mathbf{k};t=0)$. Finally, in Eq. (1) n is the number density, n $=N/V$, with V being the volume of the system (the particle diameter σ is used as the unit of length and thermodynamic limit is implied throughout). The initial value of the intermediate scattering function is equal to the static structure factor $S(k)$, $F(k;t=0)=S(k)$.

Using standard, exact but formal, methods (e.g., a projection operator approach) one can derive the following equation of motion for the intermediate scattering function:

$$\int_0^t dt' [\delta(t-t') + M^{\mathrm{irr}}(k;t-t')]\partial_{t'}F(k;t') = -\frac{D_0 k^2}{S(k)}F(k;t),$$

(3)

where D_0 is the diffusion coefficient of an isolated Brownian particle and $M^{\mathrm{irr}}(k;t)$ is the so-called irreducible [15] memory function. Within the mode-coupling approximation [11,12] applied to the system of interacting Brownian particles, the irreducible memory function is given by the following expression [13]:

$$M^{\mathrm{irr}}(k;t) = \frac{nD_0}{2}\int \frac{d\mathbf{k}_1}{(2\pi)^3}[c(k_1)\hat{\mathbf{k}}\cdot\mathbf{k}_1$$
$$+ c(|\mathbf{k}-\mathbf{k}_1|)\hat{\mathbf{k}}\cdot(\mathbf{k}-\mathbf{k}_1)]^2 F(k_1;t)F(|\mathbf{k}-\mathbf{k}_1|;t).$$

(4)

Here $\hat{\mathbf{k}}=\mathbf{k}/k$ and $c(k)$ is the so-called direct correlation function, $c(k)=[1-1/S(k)]/n$.

Substituting Eq. (4) into Eq. (3) and then differentiating the resulting equation with respect to the density, we obtain the following equation of motion for the three-point susceptibility $\chi_n(k;t)$:

$$\int_0^t dt' [\delta(t-t') + M^{\mathrm{irr}}(k;t-t')]\partial_{t'}\chi_n(k;t') + \frac{D_0 k^2}{S(k)}\chi_n(k;t)$$

$$+ nD_0\int_0^t \int \frac{d\mathbf{k}_1}{(2\pi)^3}[c(k_1)\hat{\mathbf{k}}\cdot\mathbf{k}_1 + c(|\mathbf{k}-\mathbf{k}_1|)\hat{\mathbf{k}}\cdot(\mathbf{k}-\mathbf{k}_1)]^2 \chi_n(k_1;t-t')F(|\mathbf{k}-\mathbf{k}_1|;t-t')\partial_{t'}F(k;t')$$

$$= \frac{D_0 k^2}{S^2(k)}\frac{dS(k)}{dn}F(k;t) - \frac{D_0}{2}\int_0^t dt' \int \frac{d\mathbf{k}_1}{(2\pi)^3}[c(k_1)\hat{\mathbf{k}}\cdot\mathbf{k}_1 + c(|\mathbf{k}-\mathbf{k}_1|)\hat{\mathbf{k}}\cdot(\mathbf{k}-\mathbf{k}_1)]^2 F(k_1;t-t')F(|\mathbf{k}-\mathbf{k}_1|;t-t')\partial_{t'}F(k;t')$$

$$- nD_0\int_0^t dt' \int \frac{d\mathbf{k}_1}{(2\pi)^3}[c(k_1)\hat{\mathbf{k}}\cdot\mathbf{k}_1 + c(|\mathbf{k}-\mathbf{k}_1|)\hat{\mathbf{k}}\cdot(\mathbf{k}-\mathbf{k}_1)]\left(\frac{dc(k_1)}{dn}\hat{\mathbf{k}}\cdot\mathbf{k}_1 + \frac{dc(|\mathbf{k}-\mathbf{k}_1|)}{dn}\hat{\mathbf{k}}\cdot(\mathbf{k}-\mathbf{k}_1)\right)$$

$$\times F(k_1;t-t')F(|\mathbf{k}-\mathbf{k}_1|;t-t')\partial_{t'}F(k;t').$$

(5)

We notice that the left-hand side of Eq. (5) is exactly the same as the left-hand side of the overdamped limit of the equation of motion derived by Biroli *et al.* [6] for their three-point susceptibility $\chi_\mathbf{q}(\mathbf{k};t)$ in the $\mathbf{q}\to 0$ limit. The three-point susceptibility $\chi_\mathbf{q}(\mathbf{k};t)$ is defined as the derivative of the intermediate scattering function with respect to a static, inhomogeneous external potential.

Furthermore, we recall that the derivation of the mode-coupling expression for the irreducible memory function invokes the convolution approximation for the three-point equilibrium density correlation function [13]. The convolution approximation is equivalent to assuming that the direct correlation function is density independent [16]. To be consistent, we have to use the same approximation in Eq. (5). Using $dc(k)/dn=0$ and $dS(k)/dn\equiv S^2(k)[c(k)+ndc(k)/dn] = S^2(k)c(k)$ in Eq. (5) we obtain the following equation of motion for the three-point susceptibility $\chi_n(k;t)$:

$$\int_0^t dt' [\delta(t-t') + M^{\mathrm{irr}}(k;t-t')]\partial_{t'}\chi_n(k;t') + \frac{D_0 k^2}{S(k)}\chi_n(k;t)$$

$$+ nD_0\int_0^t \int \frac{d\mathbf{k}_1}{(2\pi)^3}[c(k_1)\hat{\mathbf{k}}\cdot\mathbf{k}_1 + c(|\mathbf{k}-\mathbf{k}_1|)$$

$$\times \hat{\mathbf{k}}\cdot(\mathbf{k}-\mathbf{k}_1)]^2 \chi_n(k_1;t-t')F(|\mathbf{k}-\mathbf{k}_1|;t-t')\partial_{t'}F(k;t')$$

$$= D_0 k^2 c(k)F(k;t) - \frac{D_0}{2}\int_0^t dt' \int \frac{d\mathbf{k}_1}{(2\pi)^3}[c(k_1)\hat{\mathbf{k}}\cdot\mathbf{k}_1$$

$$+ c(|\mathbf{k}-\mathbf{k}_1|)\hat{\mathbf{k}}\cdot(\mathbf{k}-\mathbf{k}_1)]^2 F(k_1;t-t')$$

$$\times F(|\mathbf{k}-\mathbf{k}_1|;t-t')\partial_{t'}F(k;t').$$

(6)

At this point we notice that the difference between the right-hand side of Eq. (6) and the right-hand side of the equation of motion derived by Biroli *et al.* [6] for the three-point susceptibility $\chi_\mathbf{q}(\mathbf{k};t)$ in the $\mathbf{q}\to 0$ limit is a constant factor equal to $-nS(0)$. This factor is equal to the thermodynamic derivative, $-nS(0)=-(\partial n/\partial\beta\mu)_T$ where $\beta=1/(k_B T)$ and μ is the chemical potential. To rationalize this fact we notice that Biroli *et al.* used approximations which in the limit of $\mathbf{q}\to 0$ amount to $dc(k)/dn=0$. Furthermore, their three-point susceptibility is defined as the derivative of the intermediate scattering function with respect to the external potential. In the long wavelength limit, $\mathbf{q}\to 0$, this derivative differs from the derivative with respect to the density by a thermodynamic factor proportional to $(\partial n/\partial\beta\mu)_T$.

Our second object of interest is a three-point susceptibility $\chi_n^s(k;t)$ which is defined as the density derivative of the self-intermediate scattering function,

$$\chi_n^s(k;t) = \frac{dF^s(k;t)}{dn}. \tag{7}$$

Here $F^s(k;t)$ denotes the self-intermediate scattering function,

$$F^s(k;t) = \langle n_1(\mathbf{k};t)n_1(-\mathbf{k})\rangle, \tag{8}$$

where $n_1(\mathbf{k};t)$ is the Fourier transform of the microscopic density of one selected (labeled) particle at time t and $n_1(\mathbf{k}) \equiv n_1(\mathbf{k};t=0)$. The initial value of the self-intermediate scattering function is equal to 1, $F^s(k;t=0)=1$.

The derivation of the equation of motion for $\chi_n^s(k;t)$ is analogous to that for $\chi_n(k;t)$. Here we only present the starting point, i.e., the equation of motion for $F^s(k;t)$ and the final result, i.e., the equation of motion for $\chi_n^s(k;t)$. The equation of motion for the self-intermediate scattering function $F^s(k;t)$ reads

$$\int_0^t dt'[\delta(t-t') + M^{\mathrm{sirr}}(k;t-t')]\partial_{t'}F^s(k;t') = -D_0 k^2 F^s(k;t),$$
$$\tag{9}$$

where the self-irreducible memory function is given by the following expression:

$$M^{\mathrm{sirr}}(k;t) = nD_0 \int \frac{d\mathbf{k}_1}{(2\pi)^3}[c(k_1)\hat{\mathbf{k}}\cdot\mathbf{k}_1]^2 F(k_1;t)F^s(|\mathbf{k}-\mathbf{k}_1|;t).$$
$$\tag{10}$$

The equation of motion for three-point susceptibility $\chi_n^s(k;t)$ has the following form:

$$\int_0^t dt'[\delta(t-t') + M^{\mathrm{sirr}}(k;t-t')]\partial_{t'}\chi_n^s(k;t') + D_0 k^2 \chi_n^s(k;t)$$

$$+ nD_0 \int_0^t \int \frac{d\mathbf{k}_1}{(2\pi)^3}[c(k_1)\hat{\mathbf{k}}\cdot\mathbf{k}_1]^2$$

$$\times F(k_1;t-t')\chi_n^s(|\mathbf{k}-\mathbf{k}_1|;t-t')\partial_{t'}F^s(k;t')$$

$$= -D_0 \int_0^t dt' \int \frac{d\mathbf{k}_1}{(2\pi)^3}[c(k_1)\hat{\mathbf{k}}\cdot\mathbf{k}_1]^2$$

$$\times F(k_1;t-t')F^s(|\mathbf{k}-\mathbf{k}_1|;t-t')\partial_{t'}F^s(k;t')$$

$$- nD_0 \int_0^t dt' \int \frac{d\mathbf{k}_1}{(2\pi)^3}[c(k_1)\hat{\mathbf{k}}\cdot\mathbf{k}_1]^2 \chi_n(k_1;t-t')$$

$$\times F^s(|\mathbf{k}-\mathbf{k}_1|;t-t')\partial_{t'}F^s(k;t') \tag{11}$$

Note that to derive Eq. (11) we again used $dc(k)/dn=0$.

III. NUMERICAL SOLUTIONS OF EQUATIONS OF MOTION FOR $\chi_n(k;t)$ AND $\chi_n^s(k;t)$

Equations of motion (6) and (11) for the three-point susceptibilities $\chi_n(k;t)$ and $\chi_n^s(k;t)$ can be solved using the algorithm used previously [17–19] to solve mode-coupling equations (3) and (4) for the intermediate scattering function. The only input required is the structure factor $S(k)$. Here, in
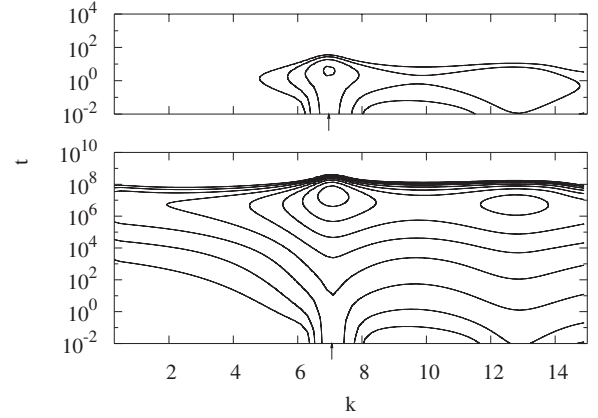

FIG. 1. Three-point susceptibility $\chi_n(k;t)$ for the reduced distance from the mode-coupling transition, $\epsilon=(\phi_c-\phi)/\phi_c=0.05$ (upper panel) and $\epsilon=10^{-4}$ (lower panel). Contours correspond to $\chi_n(k;t)=4^m$ where m is an integer, starting from $m=-1$. The arrow marks the position of the first peak of the static structure factor.

order to be consistent with earlier related work [9], we use the structure factor calculated for the hard sphere interaction potential using the Percus-Yevick closure approximation. As is customary for a mode-coupling calculation for the hard sphere system, we report the results using volume fraction $\phi=n\pi\sigma^3/6$ where σ is the hard sphere diameter or relative distance from the mode-coupling transition $\epsilon=(\phi_c-\phi)/\phi_c$.

To solve equations of motion (6) and (11) we used 300 equally spaced wave vectors from $k=0$ to $k=60$ with the first wave vector $k_0=0.1$. For this discretization of the mode-coupling equations (3) and (4) the ergodicity breaking transition (i.e., the mode-coupling transition) is located at volume fraction $\phi_c=0.515\,866\,763$ [20]. We also performed a few calculations with larger cutoffs for the integral and/or a finer grid of wave vectors and obtained qualitatively the same results.

In Figs. 1 and 2 we show $\chi_n(k;t)$ and $\chi_n^s(k;t)$, respectively, as functions of both time t and wave vector k for two different values of $\epsilon=(\phi_c-\phi)/\phi_c$, $\epsilon=0.05$ and $\epsilon=10^{-4}$. The former value of ϵ is comparable to the lowest reduced temperature $(T-T_c)/T_c$ at which mode-coupling theory agrees
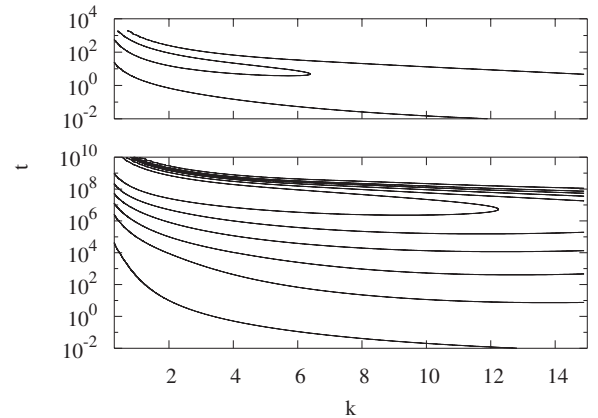

FIG. 2. Three-point susceptibility $\chi_n^s(k;t)$ for $\epsilon=0.05$ (upper panel) and $\epsilon=10^{-4}$ (lower panel). Contours correspond to $\chi_n^s(k;t)=4^m$ where m is an integer, starting from $m=-1$.

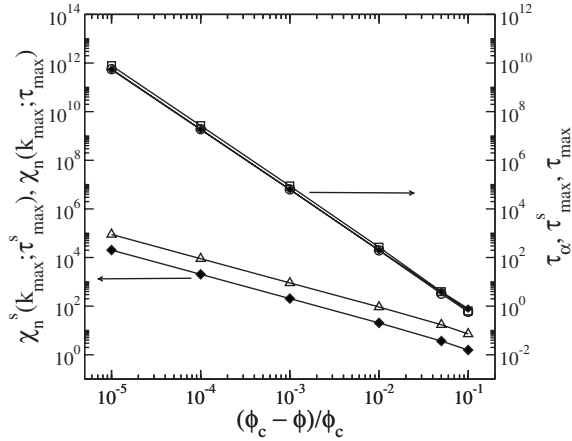FIG. 3. Right scale: dependence of the peak time of $\chi_n(k_{max};t)$ and $\chi_n^s(k_{max};t)$, τ_{max} and τ_{max}^s, respectively, and of the α relaxation time τ_α [23] on the reduced distance from the mode-coupling transition, $\epsilon = (\phi_c - \phi)/\phi_c$. Squares: τ_{max}; filled diamonds: τ_{max}^s; circles: τ_α. Left scale: dependence of the peak value of three-point susceptibilities, $\chi_n(k_{max};\tau_{max})$ and $\chi_n(k_{max};\tau_{max})$, on ϵ. Open triangles: $\chi_n(k_{max};\tau_{max})$; filled diamonds: $\chi_n^s(k_{max};\tau_{max}^s)$.

[19] with computer simulations for the well-known glass former, the Kob-Andersen Lennard-Jones binary mixture [21]. Using contour plots to show these three-point susceptibilities is inspired by a similar presentation used by Lechenault *et al.* [22] in their investigation of dynamic heterogeneity in dense, two-dimensional granular systems. One should note, however, that Lechenault *et al.* monitored and analyzed a correlation function of the fluctuations of the self-overlap integrated over the whole space. Here, we present results for three-point susceptibilities and we need to invoke the theory of Berthier *et al.* to connect these susceptibilities to dynamic heterogeneity.

We note that, as expected, the susceptibility $\chi_n(k;t)$ has a well-defined maximum at a characteristic time and wave vector. The characteristic time strongly increases upon approaching the mode-coupling transition whereas the characteristic wave vector is approximately independent of the distance from the transition and equal to 7.1 close to the transition (note that according to the Percus-Yevick approximation the first peak of the static structure factor at ϕ_c is located at $k=7.1$).

Examining Fig. 2 we note that, somewhat surprisingly, $\chi_n^s(k;t)$ does not have a well-defined maximum at a characteristic time and wave vector. In contrast with $\chi_n(k;t)$, $\chi_n^s(k;t)$ as a function of time and wave vector forms a ridge which, with decreasing wave vector, gently increases and moves towards longer times. For a fixed wave vector, e.g., for $k=k_{max}=7.1$ (i.e., the position of the first peak of the structure factor at ϕ_c), the peak position of $\chi_n^s(k;t)$ strongly increases upon approaching the mode-coupling transition.

In Fig. 3 we analyze in some detail the dependence of both three-point susceptibilities on the reduced distance from the mode-coupling transition for a fixed wave vector equal to the position of the first peak of the static structure at the transition, $k=k_{max}=7.1$. We show the dependence on $\epsilon = (\phi_c - \phi)/\phi_c$ of the time at which $\chi_n(k_{max};t)$ and $\chi_n^s(k_{max};t)$ has
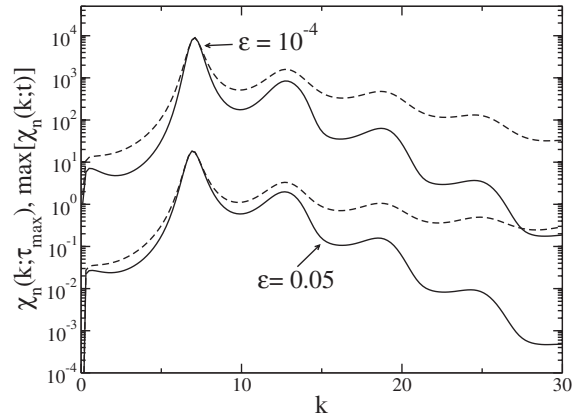

FIG. 4. Wave vector dependence of the $\chi_n(k;\tau_{max})$ (solid curves) and of the maximum value of $\chi_n(k;t)$ (dashed curves) for $\epsilon = 0.05$ (lower curves) and $\epsilon = 10^{-4}$ (upper curves).

the maximum value, τ_{max} and τ_{max}^s, respectively, and we compare these times to the α relaxation time τ_α [23]. As expected, both τ_{max} and τ_{max}^s have the same ϵ dependence as τ_α, $\tau_{max} \sim \tau_{max}^s \sim \tau_\alpha \sim \epsilon^{-2.5}$, and ratios of these times and τ_α are approximately constant, $\tau_{max}/\tau_\alpha \approx 1.4$ and $\tau_{max}^s/\tau_\alpha \approx 0.96$. In addition, we show in Fig. 3 the dependence on ϵ of the peak value of the three-point susceptibilities for a fixed wave vector $k=k_{max}=7.1$. As expected, we find $\chi_n(k_{max};\tau_{max}) \sim \chi_n^s(k_{max};\tau_{max}^s) \sim \epsilon^{-1}$.

The original motivation for investigating two-dimensional (contour) plots of $\chi_n(k;t)$ and $\chi_n^s(k;t)$ was to find the characteristic wave vector at which these susceptibilities have maximum values. Once these wave vectors have been found, one could use the theory of Berthier *et al.* to claim that at these wave vectors dynamic heterogeneities are the strongest. From this perspective, Figs. 1 and 2 lead to a rather surprising conclusion: at a fixed time comparable to the α relaxation time both $\chi_n(k;t)$ and $\chi_n^s(k;t)$ have a maximum at a nonzero wave vector. However, Fig. 2 suggests that the absolute maximum of $\chi_n^s(k;t)$ is located at or close to $k=0$. The difference between the wave vector dependence of $\chi_n(k;t)$ and $\chi_n^s(k;t)$ is investigated in some detail in Figs. 4 and 5. In the former figure we compare the wave vector dependence of $\chi_n(k;\tau_{max})$ [recall that τ_{max} is the peak position of $\chi_n(k_{max};t)$] with the wave vector dependence of the maximum value of $\chi_n(k;t)$ for two different values of $\epsilon = (\phi_c - \phi)/\phi_c$, $\epsilon = 0.05$, and $\epsilon = 10^{-4}$. We notice that the wave vector dependence is quite strong but qualitatively similar, except for higher wave vectors. In Fig. 5 we show the wave vector dependence of $\chi_n^s(k;\tau_{max})$ [τ_{max}^s is the peak position of $\chi_n^s(k_{max};t)$] with the wave vector dependence of the maximum value of $\chi_n^s(k;t)$ for the same two different values of ϵ. We see that in this case the wave vector dependence is quite a bit weaker than that shown in Fig. 4. More importantly, we see that the wave vector dependence of $\chi_n^s(k;\tau_{max})$ and of the maximum value of $\chi_n^s(k;t)$ are qualitatively different.

It is useful to examine whether the rather strong wave vector dependence of the maximum value of $\chi_n(k;t)$ and the monotonic wave vector dependence of the maximum value of $\chi_n^s(k;t)$ originate from the wave vector dependence of the transient structure. To this end we recall that within the
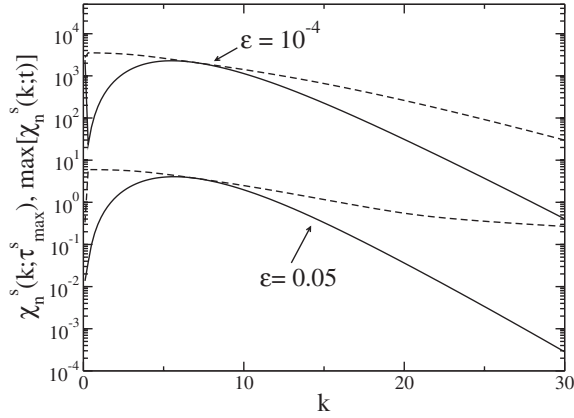
FIG. 5. Wave vector dependence of the $\chi_n^s(k;\tau_{max}^s)$ (solid curves) and of the maximum value of $\chi_n^s(k;t)$ (dashed curves) for $\epsilon=0.05$ (lower curves) and $\epsilon=10^{-4}$ (upper curves).

mode-coupling theory in the α relaxation regime one can derive the following scaling laws for the collective and self-intermediate scattering functions [11]:

$$F(k;t) = A(k)g_\alpha(k;t/\tau_\alpha), \tag{12}$$

$$F^s(k;t) = A^s(k)g_\alpha^s(k;t/\tau_\alpha^s). \tag{13}$$

In Eq. (12) $A(k)$ is a wave-vector-dependent height of the plateau in the collective intermediate scattering function and $g_\alpha(k;t)$ is a scaling function which may depend on wave vector but is independent of density (more generally, independent of the control parameter). The plateau height is density independent and it is given by the product of the static structure factor at the transition and the nonergodicity parameter $f(k)$ at the transition, $A(k)=S(k;\phi_c)f(k;\phi_c)$ [note that we indicated the volume fraction dependence of $S(k)$ and $f(k)$ to emphasize that they are to be evaluated at a fixed volume fraction]. The quantities in Eq. (13) have a similar meaning except that $A^s(k)=f^s(k;\phi_c)$. The scaling behavior (12) and (13) is only predicted to hold close to the transition temperature and for times around the α relaxation time. Note that since both the prefactors and the scaling functions in Eqs. (12) and (13) are density independent, three-point susceptibilities are intimately related to the increase of the α relaxation time with increasing density [8,9]. The scaling (12) and (13) suggests that since there is considerable structure observed in the wave vector dependence of $A(k)$, but $A^s(k)$ is a monotonically decreasing function of the wave vector [11]. Thus the qualitative difference between the wave vector dependence of the maximum values of $\chi_n(k;t)$ and $\chi_n^s(k;t)$ may be due to the prefactors in Eqs. (12) and (13). To examine this possibility we looked at the maximum value of $\chi_n(k;t)/A(k)$ and $\chi_n^s(k;t)/A^s(k)$ as a function of k, Fig. 6. We note that while dividing by the prefactors $A(k)$ and $A^s(k)$ removes most of the wave vector dependence, there is still a peak in the maximum value of $\chi_n(k;t)/A(k)$, but this peak does not exist in $\chi_n^s(k;t)/A^s(k)$.

Finally, in Fig. 7 we show that upon approaching the mode-coupling transition three-point susceptibility $\chi_n(k_{max};t)$ approaches the scaling limit. The three point sus-
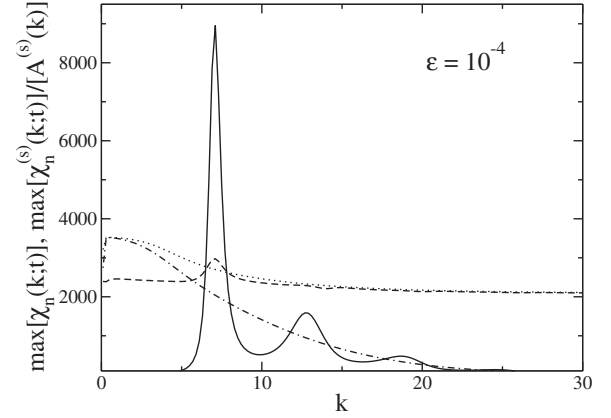

FIG. 6. Wave vector dependence of the maximum value of $\chi_n(k;t)$ (dashed line) compared to that of the maximum value of $\chi_n(k;t)/A(k)$ (solid line), and wave vector dependence of the maximum value of $\chi_n^s(k;t)$ (dash-dot line) compared to that of the maximum value of $\chi_n^s(k;t)/A^s(k)$ (dotted line) for $\epsilon=10^{-4}$.

ceptibility $\chi_n^s(k_{max};t)$ also approaches the scaling limit, but in a somewhat more complicated way (not shown). The inset in Fig. 7 shows the time dependence of $\chi_n^s(k_{max};t)$ for a small value of ϵ equal to 10^{-6}. Comparison of the main figure and the inset shows that upon approaching the mode-coupling transition the time dependence of both susceptibilities at $k=k_{max}$ is quite similar.

IV. DISCUSSION

The main reason for our interest in three-point susceptibilities $\chi_n(k;t)$ and $\chi_n^s(k;t)$ was the connection between these susceptibilities and four-point correlation functions which quantify dynamic heterogeneities. Roughly speaking, according to Berthier *et al.* [8,9], the Brownian system's four-point correlation function $\chi_4(k;t)$, which is defined as the self part of the four-point dynamic density correlation function inte-
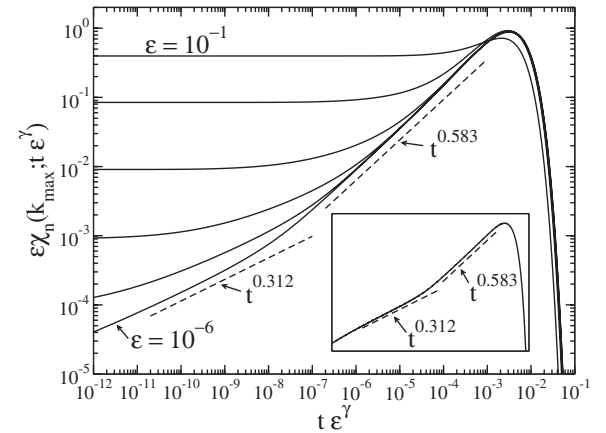

FIG. 7. Scaling plot of $\chi_n(k_{max};t)$. Solid lines correspond to ϵ equal to 10^{-1}, $10^{-2}, 10^{-3}$, 10^{-4}, 10^{-5}, and 10^{-6} (top to bottom). Inset: time dependence of $\chi_n^s(k_{max};t)$ at a very small value of $\epsilon=10^{-6}$. Dashed lines in the main figure and in the inset indicate transient power law dependence in the early and late β regimes.

grated over the whole space, is proportional to $\chi_n^s(k;t)^2$ for a system in which the total number of particles can fluctuate and is proportional to $\chi_n^s(k;t)$ for a system with fixed total number of particles (note that the latter one is commonly used in numerical simulations). Following Berthier *et al.* and assuming that mode-coupling theory gives at least qualitatively correct results for three-point susceptibility $\chi_n^s(k;t)$ we are faced with a striking conclusion that there is no finite *intrinsic* [24] wave vector at which dynamic heterogeneities, as quantified by $\chi_4(k;t)$, are the largest. More precisely, at a fixed time we can determine a finite characteristic wave vector, but with increasing time this wave vector is decreasing towards 0. In other words, the maximum value of $\chi_4(k;t)$ is predicted to monotonically decrease with increasing k.

The wave vector dependence of four-point correlation function $\chi_4(k;t)$ was monitored in two recent simulational investigations [24,25]. Both studies used Newtonian rather than Brownian dynamics and thus our findings cannot be directly compared to their results. However, it is interesting to note that Ref. [25] found that the time at which $\chi_4(k;t)$ reaches its maximum value increases as the wave vector decreases from the peak position of the structure factor, in rough agreement with Fig. 2. The authors of Ref. [25] did not comment on the dependence of the maximum value of $\chi_4(k;t)$ on the wave vector but from their Fig. 1 it seems that it does not increase with decreasing wave vector, in contrast to our Figs. 2 and 5. The second study, Ref. [24], shows the dependence of the maximum value of $\chi_4(k;t)$ [26] on the wave vector. It exhibits a broad maximum located at a wave vector slightly smaller than the peak position of the static structure factor. Qualitatively, this disagrees with our results shown in Figs. 2 and 5. At present, the origin of the differences between our findings and the results of Refs. [24,25] is unclear.

In closing, we would like to emphasize that various four-point functions quantifying dynamic heterogeneities have been studied in computer simulations for more than a decade. On the other hand, theoretical predictions for these functions started to appear only in the last few years. Quantitative comparison between simulations and theories is still in infancy. We hope that this work will stimulate further effort in this direction.

[1] For reviews of experimental evidence of dynamic heterogeneities see, e.g., M. Ediger, Annu. Rev. Phys. Chem. **51**, 99 (2000); R. Richert, J. Phys.: Condens. Matter **14** R703 (2002). For a recent review of simulational evidence, see H. C. Andersen, Proc. Natl. Acad. Sci. U.S.A. **102**, 6686 (2005).

[2] C. Donati, S. Franz, S. C. Glotzer, and G. Parisi, J. Non-Cryst. Solids **307-310**, 215 (2002).

[3] S. Franz and G. Parisi, J. Phys.: Condens. Matter **12**, 6335 (2000).

[4] G. Biroli and J.-P. Bouchaud, Europhys. Lett. **67**, 21 (2004).

[5] L. Berthier *et al.*, Science **310**, 1797 (2005).

[6] G. Biroli, J.-P. Bouchaud, K. Miyazaki, and D. R. Reichman, Phys. Rev. Lett. **97**, 195701 (2006).

[7] M. Iwata and S. Sasa, Europhys. Lett. **77**, 50008 (2007).

[8] L. Berthier *et al.*, J. Chem. Phys. **126**, 184503 (2007).

[9] L. Berthier *et al.*, J. Chem. Phys. **126**, 184504 (2007).

[10] G. Szamel, Phys. Rev. Lett. **101**, 205701 (2008).

[11] W. Götze, in *Liquids, Freezing and Glass Transition*, edited by J. P. Hansen, D. Levesque, and J. Zinn-Justin (North-Holland, Amsterdam, 1991).

[12] S. P. Das, Rev. Mod. Phys. **76**, 785 (2004).

[13] For the derivation of mode-coupling theory equations for the colloidal system, see G. Szamel and H. Löwen, Phys. Rev. A **44**, 8215 (1991).

[14] For a comparison of the complete four-point function and its self part see, e.g., N. Lačević, F. W. Starr, T. B. Schrøder, and S. C. Glotzer, J. Chem. Phys. **119**, 7372 (2003).

[15] B. Cichocki and W. Hess, Physica A **141**, 475 (1987).

[16] J.-L. Barrat, J.-P. Hansen, and G. Pastore, Phys. Rev. Lett. **58**, 2075 (1987).

[17] M. Fuchs, W. Götze, I. Hofacker, and A. Latz, J. Phys.: Condens. Matter **3**, 5047 (1991).

[18] K. Miyazaki, B. Bagchi, and A. Yethiraj, e-print arXiv:cond-mat/0405326v1; Note that the published version of this manuscript [J. Chem. Phys. **121**, 8120 (2004)] does not contain the detailed description of the numerical algorithm.

[19] E. Flenner and G. Szamel, Phys. Rev. E **72**, 031508 (2005).

[20] U. Bengtzelius, W. Götze, and A. Sjölander, J. Phys. C **17**, 5915 (1984).

[21] W. Kob and H. C. Andersen, Phys. Rev. Lett. **73**, 1376 (1994); Phys. Rev. E **51**, 4626 (1995); **52**, 4134 (1995).

[22] F. Lechenault, O. Dauchot, G. Biroli, and J.-P. Bouchaud, Europhys. Lett. **83**, 46003 (2008).

[23] The α relaxation time τ_α is defined as the time at which the intermediate scattering function $F(k;t)$ at the wave vector corresponding to the first peak of the static structure factor is equal to e^{-1}, $F(k_{\max};\tau_\alpha)=e^{-1}$.

[24] P. Charbonneau and D. R. Reichman, Phys. Rev. Lett. **99**, 135701 (2007).

[25] D. Chandler, J. P. Garrahan, R. L. Jack, L. Maibaum, and A. C. Pan, Phys. Rev. E **74**, 051501 (2006).

[26] Note that the definition of $\chi_4(k;t)$ used in Ref. [24] is somewhat nonstandard.